Bulletin of Environmental Contamination and Toxicology (2021) 106:409–414
https://doi.org/10.1007/s00128-020-02843-8

Continuous Flow Process for Cr(VI) Removal from Aqueous Solutions Using Resin Supported Zero-Valent Iron

A. Toli[1] · Ch. Mystrioti[1] · A. Xenidis[1] · N. Papassiopi[1]

Received: 17 February 2020 / Accepted: 30 March 2020 / Published online: 16 April 2020

Abstract

The objective of the present study was to evaluate the performance of a nanocomposite material consisting of nano zero valent iron and a cation exchange resin, for the reduction of chromate, by conducting column tests. A cationic resin, Amberlyst 15, was selected as porous host material. The synthesis of the nanocomposite material (R-nFe) was carried out using Green Tea extract to obtain the reduction of adsorbed Fe(III) to the elemental state Fe(0). Three column tests were implemented with different dimensions, corresponding to variable contact times between the aqueous solution and the resin beads loaded with Fe(0), namely 168, 744 and 1260 s respectively for columns I, II and III. The results indicated that the removal of Cr(VI) follows a first order kinetic law with a chemical constant equal to 0.0526 min^{-1} (8.8×10^{-4} s^{-1}).

Keywords nZVI nanocomposite · Macroreticular resin support · Chromate reduction · Continuous flow tests

Chromate is an environmental contaminant which is commonly detected in groundwater and in drinking waters. Cr(VI) and Cr(III) are the most stable oxidation forms of chromium which occur in the environment. Trivalent chromium presents limited solubility and at low doses is considered an essential nutrient element for metabolism. Contrary, hexavalent chromium is accused to be highly toxic ($HCrO_4^-$, CrO_4^{2-}) and soluble. Despite the toxicity of hexavalent chromium, it is used in many industrial applications such as in metal electroplating, in wood preservation, in leather tanning and in pigments and dyes. Concentrations of hexavalent chromium can be detected in the environment accidently or due to inefficient waste treatment from industries. The most common technologies for water treatment for the Cr(VI) remediation are the chemical reduction and precipitation, adsorption, ion exchange, membrane filtration, biological and electrochemical remediation. Iron and sulphur based compounds are used as agents for the chemical reduction of Cr(VI) to Cr(III) (Chrysochoou et al. 2012; Di Palma et al. 2015). Nano ZVI is more efficient compared to micro or millimeter scale ZVI, due to the small particle size, large specific surface area and high reactivity (O'Carroll et al. 2013; Bavasso et al. 2016). Nanoscale ZVI is mainly applied for in-situ injection (Mystrioti et al. 2018). The use of nano zero valent iron (nZVI) for the reduction of Cr(VI) in the presence of selected other heavy metals was proved to be fast and efficient (Gueye et al. 2016).

However, nZVI presents limited mobility to calcareous aquifers and may be toxic for living organisms or cells. The incorporation of nZVI to inert materials are currently under investigation. In this category of technologies iron nanoparticles are fixed on a permeable matrix and this composite material is applied for the treatment of contaminated waters under flow conditions, such as a permeable wall underground or an appropriate filter in above ground installations. Solid porous materials, such as carbon, resins, zeolite etc., have been tested as support material for nZVI (Fu et al. 2014). The support material protects iron nanoparticles from rapid oxidation, hydrolysis in water and agglomeration. Cation exchange resins can be efficiently used as a chemically inert medium, which simultaneously combines the chemical and the physical binding of iron nanoparticles without affecting their reactivity and allow the distribution of the pollutants through the porous matrix of the resin. Moreover cationic resins as supporting matrix can retain Fe(III) and Cr(III), which are produced during the chemical reaction between nZVI and Cr(VI).

Studies involving the synthesis of resin supported nZVI are limited in number (Shu et al. 2010; Fu et al. 2013; Xie

✉ A. Toli
katerinatoli@metal.ntua.gr

[1] Sch. of Mining and Metallurgical Eng., National Technical University of Athens, 15780 Athens, Greece

et al. 2014; Toli et al. 2016, 2018). The usual synthesis procedure includes two steps. The first step consists in the adsorption of Fe(III) or Fe(II) cations and the second step involves the reduction of adsorbed iron by an appropriate reducing agent. In the majority of published researches reduction is carried out using $NaBH_4$. In previously published studies we have demonstrated that the reduction of adsorbed ferric cations can be successfully carried out using synthetic or natural polyphenols as "green" alternative to the borohydride (Toli et al. 2016, 2018).

A nanocomposite material, combining the macroporous resin Amberlyst 15 as host material and green tea extract as reductant of Fe(III), was synthesized and evaluated for the removal of Cr(VI) from contaminated waters by conducting batch tests (Toli et al. 2018). The aim of the present study was to evaluate the performance of this nanocomposite material for the treatment of Cr(VI) contaminated waters under flow conditions.

Materials and Methods

The synthesis of resin-nZVI nanocomposite was carried out as described in Toli et al. (2018), using Amberlyst 15 H^+ (Sigma-Aldrich, China) as host matrix, iron chloride ($FeCl_3 \cdot 6H_2O$) as source of iron and dry leaves of green tea (Twinings of London) as source of polyphenols. The loading of resin with nanoiron was equal to 0.5 mmol per gram (mol/kg). Potassium bromide (KBr) was used as tracer during the column tests and potassium dichromate ($K_2Cr_2O_7$) was used for the simulation of chromate contaminated waters.

Three column tests were carried out with the R-nFe beads, using polyethylene columns with different dimensions, corresponding to variable contact times between the aqueous solution and the resin, namely 168, 744 and 1260 s respectively for Columns I, II and III. An additional column IV, with dimensions similar to column II, was prepared using silica sand instead of resin beads. Column V was used as a control experiment to evaluate the differences between the transport properties of ionic species, when they are moving through a bed of resin beads, with extended internal porosity, or through a bed of compact grains, like the silica sand. The characteristics of the four columns are presented in Table 1. The R-nFe and the silica sand were placed manually and gently vibrated at several stages to ensure uniform packing. Additionally, thin layers of fiber glass were used at the inlet and outlet of the columns to distribute the flow over the cross-sectional area of the fixed-bed column. Each packed column was connected to a peristaltic pump (Alitea, Sweden) and to a reservoir, which contained the fluids prepared for introduction in the column. Introduction of fluids was carried out in an upflow mode with flow rate equal to 2×10^{-8} m^3/s. The packed columns were first saturated with deionized water (DW) to obtain a steady flow rate. As seen in Table 1, the Reynolds numbers describing the flow regime through packed beds, Re_b, have values varying between 0.02

Table 1 Properties and operating conditions of columns

Parameter	R-nFe columns			Sand column
	I	II	III	IV
Resin (or silica sand) mass, M ($kg \times 10^{-3}$)	9	37.92	81.57	79.5
Column diameter, d ($m \times 10^{-2}$)	1.6	2.63	2.63	2.63
Bed height, L ($m \times 10^{-2}$)	5.2	8.2	16.4	8.6
Bed Volume, BV ($m^3 \times 10^{-6}$)	10.5	44.5	89.1	46.7
Particle density, ρ_p (kg/m^3)[a]	1278	1278	1278	2503
Mean particles diameter, d_p ($m \times 10^{-6}$)	745	745	745	400
Bulk density, ρ_b (kg/m^3)[b]	861	851	916	1702
External porosity, θ[c]	0.326	0.334	0.283	0.319
Pore volume size, V_{PV} ($m^3 \times 10^{-6}$)[d]	3.41	14.88	25.27	14.92
Solution flowrate, Q ($m^3/s \times 10^{-8}$)	2	2	2	2
Pore velocity, v ($m/s \times 10^{-4}$)[e]	3.03	1.10	1.30	1.15
Reynolds for flow around particles, Re_p[f]	0.0823	0.0304	0.0305	0.0163
Reynolds for flow through packed bed, Re_b[g]	0.122	0.0457	0.0425	0.0239

[a]Particle density: determined based on Archimedes' principle

[b]Bulk density: $\rho_b = M/BV$

[c]External porosity: $\theta = 1 - \rho_b/\rho_p$

[d]$V_{PV} = BV * \theta$

[e]$v = Q \Big/ \left(\theta \times \frac{\pi d^2}{4}\right)$

[f]$Re_p = v\theta d_p/\nu$,

[g]$Re_b = Re_p/(1-\theta)$, where $\nu = 9 \times 10^{-7}$ m^2/s water kinematic viscosity at 25 °C

and 0.12, which indicate laminar flow conditions (Fogler 2006). Afterwards a solution of KBr, with initial concentration of Br equal to 1 mol/m^3, was introduced in the columns. The objective of this step was to study the transport properties of an inert anion, like Br, during its movement through the R-nFe bed. Finally a solution simulating Cr(VI) contaminated groundwater, with concentration 5 mg/L (0.096 mol/m^3), was introduced in the columns. The concentration of Br in the effluents was determined using an ion-selective electrode, according to the USEPA method 9211. Chromate was determined spectroscopically by the carbazide method, using a UV–Vis spectrophotometer Hitachi (U1100).

Results and Discussion

Bromide is an anion not expected to react chemically with the elemental iron retained inside the R-nFe beads. The transport of bromide was studied in order to evaluate the mobility of an inert anion through the columns without the interference of chemical reaction. The results are presented in Fig. 1. Axis X corresponds to the duration of flow, t, and is related with the cumulative amount of solution (V), or the number of pore volumes (N_{PV}) passing through the bed, according to Eq. (1):

$$t = \frac{V}{Q} = \frac{N_{PV} V_{PV}}{Q} \tag{1}$$

where Q is the volumetric flowrate and V_{PV} is the size of pore volume.

The transport was described applying the classic 1-D Convection Dispersion Equation (CDE) (Eq. 2):

$$R\frac{\partial C}{\partial t} = D\frac{\partial^2 C}{\partial z^2} - v\frac{\partial C}{\partial z} - k'C \tag{2}$$

$$R = 1 + \frac{\rho_b K_d}{\theta} \tag{3}$$

$$K_d = \frac{C_s}{C} \tag{4}$$

where C (10^3 mol/m^3) is the concentration of the studied component in the aqueous phase, v (2×10^{-4} m/s) is the pore velocity of the fluid, D (2×10^{-6} m^2/s) is the hydrodynamic dispersion coefficient, R is the retardation factor, K_d (10^{-3} m^3/kg) is the distribution coefficient of the studied component between the aqueous phase and the solids, C_s (mol/kg) is the concentration of component on the solids. The term $-k'C$ in Eq. (2) describes the disappearance of component due to a chemical reaction, assuming a first order reaction.

The calculations were carried out using the CXTFIT code of STANMOD software (Simunek et al. 2003). When there is no mechanism able of retaining a soluble component on the bed solids, the distribution coefficient K_d is equal to zero and the retardation factor R becomes equal to 1. In this case, the breakthrough curve can be described using as fitting parameter only the axial dispersion D. This is the case of column IV, where the bed consists of sand particles (Fig. 1a). Column II had similar dimensions with the sand column (see Table 1), but the breakthrough of Br appeared with relative delay and the curve presented a higher slope (Fig. 1a). To describe the transport through this column it was necessary to introduce a value of R greater than 1, namely R = 1.91. Similarly for Columns I and III, the best

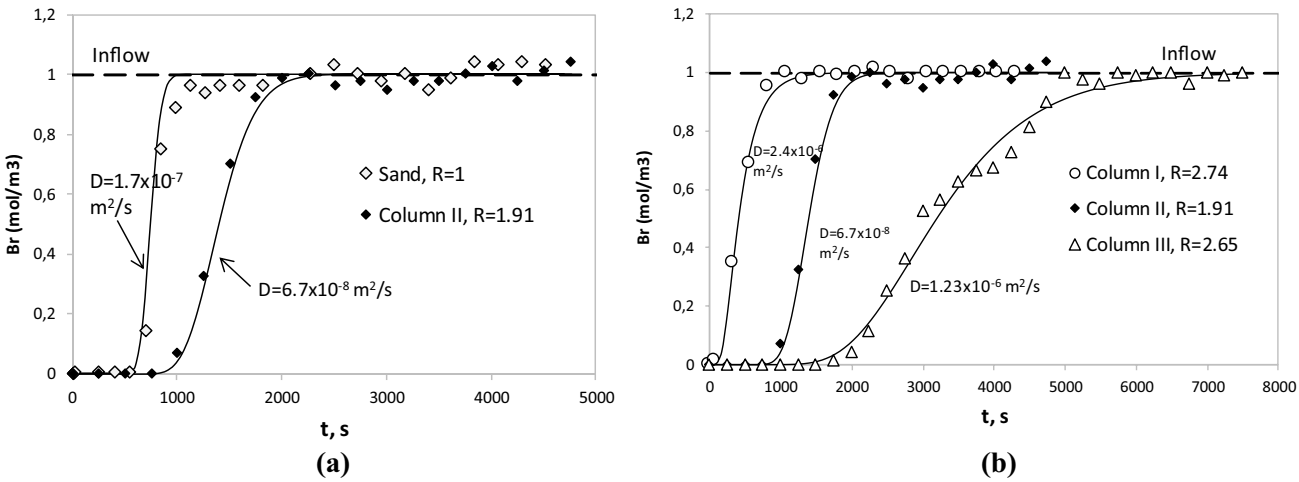

Fig. 1 Comparison of Br breakthrough curves (**a**) through columns of similar dimensions filled with sand and RnFe nanocomposite and (**b**) through Columns I II and III with different dimensions and filled with R-nFe. Continuous lines were calculated using the 1-D CDE model

fitting of experimental data was obtained with R = 2.74 and R = 2.65 respectively.

The K_d values corresponding to the retardation factors of the three R-nFe columns, were calculated from Eq. (3), and found equal to 0.66, 0.37 and 0.51 ($\times 10^{-3}$ m^3/kg). From Eq. (4) we can also calculate the amount of Br retained by the R-nFe beads. Given that the concentration of Br in the aqueous phase is equal to 1 mol/m^3, the corresponding concentration on the solids, C_s, is equal to 0.66, 0.37 and 0.51 ($\times 10^{-3}$ mol/kg), for Columns I, II and III respectively.

Amberlyst 15 is a cationic resin and is not expected to retain anions. On the other hand elemental iron, Fe(0), has no effect on Br^-. A possible mechanism explaining the partial retention of Br by the resin is that Br anions are simply transferred by diffusion and entrapped inside the internal macro- and micropores of resin beads. It is noted that the retention of Br anions is negligible compared to the cation exchange capacity of the resin, which was found equal to 1.83 eq/kg (Toli et al. 2018), i.e. more than 2500 higher compared to the retention of Br.

The breakthrough curves of Cr(VI) in Columns I, II and III are presented in Fig. 2. As seen in the figure after an initial transient period, the concentration of Cr(VI) in the effluent reaches a plateau which is equal to 0.083 mol/m^3 of Cr(VI) in column I, 0.050 mol/m^3 in column II and 0.036 mol/m^3 in column III. This value is by 0.013 mol/m^3, 0.046 mol/m^3 and 0.060 mol/m^3 lower compared to the concentration of Cr(VI) in the feed solution, i.e. 0.096 mol/m^3. The appearance of this plateau indicates a kinetic limitation for the reduction of Cr(VI) to the Cr(III) state during the flow of the solution through the 3 columns. The concentration in the effluent, C_{ef}, is related with the concentration in the influent, C_{in}, according to Eq. (5):

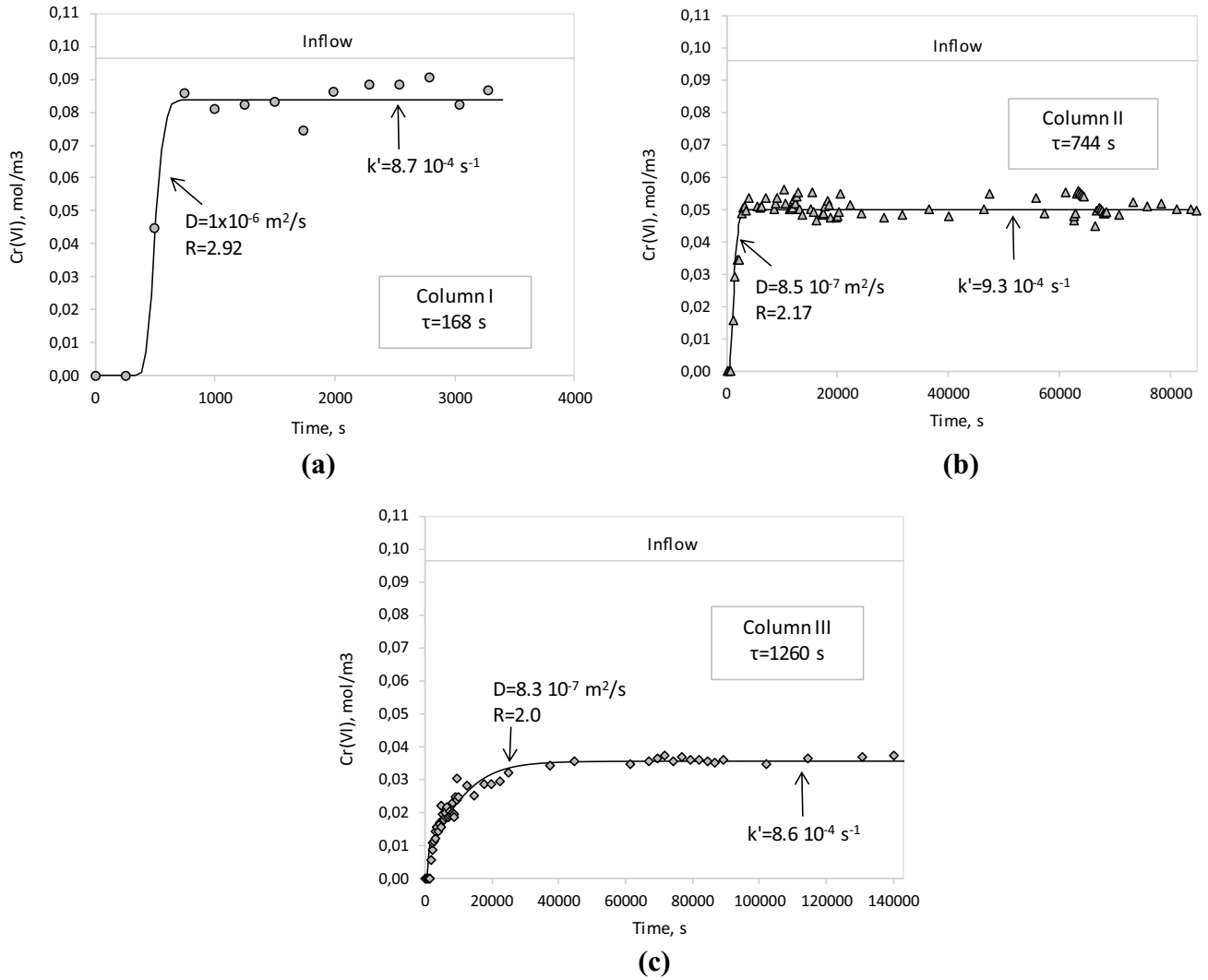

Fig. 2 Breakthrough curves of Cr(VI) through Columns I (**a**), II (**b**) and III (**c**). Continuous lines were calculated using 1-D CDE model

$$ln\left(\frac{C_{ef}}{C_{in}}\right) = -k'\tau \quad (5)$$

$$\tau = \frac{V_{PV}}{Q} \quad (6)$$

where k' is the rate constant of the pseudo-first order kinetic law (see also Eq. 2), and τ is the residence time of solution in contact with the R-nFe beads inside the columns. The residence time τ was calculated from Eq. (6) taking into consideration the characteristics of the three columns (see Table 1), and was found equal to 168, 744 and 1260 s for columns I, II and III respectively.

The value of rate constant k' was calculated from Eq. (5) and was found equal to 8.4×10^{-4} s^{-1} for column I, 9.3×10^{-4} s^{-1} for Column II and 8.6×10^{-4} s^{-1} for column III. The three values of k' are very close supporting the assumption of first order kinetic with respect to Cr(VI). Based on these experiments, the mean value and the standard deviation of this rate constant is $k' = (8.8\pm0.38)\times10^{-4}$ s^{-1}. It is noted that the amount of elemental Fe(0) in the three columns is in high stoichiometric excess with respect to the Cr(VI) supplied in the feed solutions. Namely the total mass of Fe(0) corresponds to 4.56, 19.23 and 41.37 (10^{-3} mol), while total Cr(VI) introduced in the columns was less than 0.01, 0.17 and 0.29 (10^{-3} mol). As a consequence, depletion of elemental iron is not expected to interfere with the observed kinetics. Column effluents were sampled and analyzed for pH. The pH of Cr(VI) solution in the inflow was 4.9. The pH of effluent solutions remained quasi constant during the tests, namely close to 4.5, 4.8 and 5.5 for Columns I, II and III respectively.

The performance of the process under flow conditions through the columns is lower compared to what was expected from the batch experiments carried out with the same nanocomposite material (Toli et al. 2018). In this work it was found that the reaction can be described with a kinetic law of 1st order with respect to the concentration of Cr(VI) and that the kinetic constant k_1 is proportional to the amount of nanoiron, as expressed by Eq. (7):

$$k_1 = k_2\frac{C_{SnFe}M_R}{V} \quad (7)$$

where C_{SnFe} is the moles of nFe per unit mass of RnFe, M_R the mass of RnFe and V the volume of aqueous solution. The constant k_2 was found to vary in the range 0.83×10^{-5}–7.67×10^{-5} $(mol/m^3)^{-1}/s^{-1}$. In the case of column experiments, the volume of aqueous phase is equal to the pore volume, V_{PV}, and the mass M_R is the amount of resin inside each column (see Table 1). The content of nanoiron in the resin beads (C_{SnFe}) was equal to 0.5 mol/kg for all the columns. Applying Eq. (7), with $k_2 = 4.17\times10^{-5}$ $(mol/m^3)^{-1}$ s^{-1}, it is calculated that the kinetic constant k_1 should range between 0.053 and 0.067 s^{-1}, depending on the different packing of RnFe beads in the columns. These values are approximately 60–75 times higher compared to the experimental $k' = 8.8\times10^{-4}$ s^{-1}. The lower kinetics during the column experiments indicates that there is an additional resistance, which is not interfering when the reaction takes place in an agitated suspension. This resistance may be related to the mass transfer of Cr(VI) from the bulk liquid to the external surface of the beads, a process which is usually negligible under agitated conditions, but may become important under flow conditions through a packed bed.

There are very few studies investigating the kinetics of Cr(VI) removal under flow conditions, using nZVI fixed on porous media. A recent study is that of Fan et al. (2019), who synthesized a nanocomposite consisting of nZVI supported on a biochar matrix. From the column experiments, they determined a first order kinetic constant varying between 0.61 and 0.58 h^{-1} (0.61×10^{-4}–1.61×10^{-4} s^{-1}), which is about 10 times lower compared to our study. Also Vilardi et al. (2018) used olive stones as the support of zero-valent iron and magnetite nanoparticles to develop a new material for the removal of chromium, organic matter and total phenols from wastewater. They determine the Cr(VI) removal process as a combination of sorption, reduction and co-precipitation phenomena.

Chromium (VI) concentrations in the order of 100 µg/L have been detected in several aquatic bodies in Greece, and there is strong evidence that these levels may be primarily related to geogenic processes (Dermatas et al. 2015; Pyrgaki et al. 2019; Vasileiou et al. 2019). On the other hand contamination levels as high as 11.7 mg/L have been reported in the highly industrialized area of Oinofyta and are obviously related with anthropogenic activities (Pyrgaki et al. 2019). Assuming a fixed bed installation filled with the R-nFe nanocomposite material, and setting as remediation goal to decrease the concentration of Cr(VI) below the level of 10 µg/L, we can calculate that the aqueous stream should remain in contact with R-nFe for 44 or 135 min, if the initial Cr(VI) concentration is 100 or 12,000 µg/L respectively (Eq. 5). These levels of contact time are high for a conventional filter, but can be considered as probable if R-nFe is used for the operation of a permeable reactive barrier. Namely, if groundwater flows with a velocity equal to 1 m/day and passes through a barrier filled with R-nFe and having a thickness of 0.5 m, the contact time would be more than 200 min, a time sufficient for obtaining the desired low levels of Cr(VI).

However there many other aspects, which may affect the performance of this nanocomposite material, such as the effect of coexisting anions and cations, and require further investigation.

In the present study, a composite material, consisting of nanoscale Fe(0) dispersed in the cationic resin Amberlyst 15, was synthesized, using green tea extract for the reduction of adsorbed Fe(III). The effectiveness of this composite material in remediating Cr(VI) contaminated waters was evaluated by conducting column tests. The results of column tests indicated that the removal of Cr(VI) follows a first order kinetic law and the value of the kinetic constant was found equal to 0.0526 min^{-1} (k'=8.8 10^{-4} s^{-1}). Based on these results it was calculated that a PRB, with 0.5 m thickness and filled with this nanocomposite material, can achieve the clean-up of contaminated groundwater by reducing Cr(VI) concentration to safe levels, i.e. below 10 µg/L, even if the initial contamination is very high, in the order of 12,000 µg/L.

References

Bavasso I, Vilardi G, Stoller M et al (2016) Perspectives in nanotechnology based innovative applications for the environment. Chem Eng 47:55–60. https://doi.org/10.3303/CET1647010

Chrysochoou M, Johnston CP, Dahal G (2012) A comparative evaluation of hexavalent chromium treatment in contaminated soil by calcium polysulfide and green-tea nanoscale zero-valent iron. J Hazard Mater 201–202:33–42. https://doi.org/10.1016/j.jhazmat.2011.11.003

Dermatas D, Mpouras T, Chrysochoou M et al (2015) Origin and concentration profile of chromium in a Greek aquifer. J Hazard Mater 281:35–46. https://doi.org/10.1016/j.jhazmat.2014.09.050

Di Palma L, Gueye MT, Petrucci E (2015) Hexavalent chromium reduction in contaminated soil: A comparison between ferrous sulphate and nanoscale zero-valent iron. J Hazard Mater 281:70–76. https://doi.org/10.1016/j.jhazmat.2014.07.058

Fan Z, Zhang Q, GaO B, Liu C, Qiu Y (2019) Removal of hexavalent chromium by biochar supported nZVI composite: Batch and fixed-bed column evaluations, mechanisms, and secondary contamination prevention. Chemosphere 217:85–94

Fogler HS (2006) Elements of chemical reaction Engineering Bioprocess Engineering. Prentice Hall PTR, Upper Saddle River

Fu F, Ma J, Xie L et al (2013) Chromium removal using resin supported nanoscale zero-valent iron. J Environ Manage 128:822–827. https://doi.org/10.1016/j.jenvman.2013.06.044

Fu FL, Dionysiou DD, Liu H (2014) The use of zero-valent iron for groundwater remediation and wastewater treatment: a review. J Hazard Mater 267:194–205. https://doi.org/10.1016/j.jhazmat.2013.12.062

Gueye T, Di Palma L, Gunel A et al (2016) The influence of heavy metals and organic matter on hexavalent chromium reduction by nano zero valent iron in soil. Chem Eng Trans 47:289–294. https://doi.org/10.3303/CET1647049

Mystrioti C, Toli A, Papasiopi N et al (2018) Chromium removal with environmentally friendly iron nanoparticles in a Pilot Scale Study. Bull Environ Contam Toxicol. https://doi.org/10.1007/s00128-018-2424-3

O'Carroll D, Sleep B, Krol M et al (2013) Nanoscale zero valent iron and bimetallic particles for contaminated site remediation. Adv Water Resour 51:104–122. https://doi.org/10.1016/j.advwatres.2012.02.005

Pyrgaki K, Argyraki A, Kelepertzis S et al (2019) A DPSIR approach to selected Cr(VI) impacted groundwater bodies within Attica and Eastern Sterea Ellada River Basin Districts. In: 16th International Conference on Environmental Science and Technology.

Shu HY, Chang MC, Chen CC, Chen PE (2010) Using resin supported nano zero-valent iron particles for decoloration of Acid Blue 113 azo dye solution. J Hazard Mater 184:499–505. https://doi.org/10.1016/j.jhazmat.2010.08.064

Simunek J, Genuchten TM, Sejna M, Toride N, Leij FJ (2003) STANMOD, (STu-dio of ANalytical MODels). version 2.08.1130

Toli A, Chalastara K, Mystrioti C et al (2016) Incorporation of zero valent iron nanoparticles in the matrix of cationic resin beads for the remediation of Cr(VI) contaminated waters. Environ Pollut 214:419–429. https://doi.org/10.1016/j.envpol.2016.04.034

Toli A, Varouxaki A, Mystrioti C et al (2018) Green synthesis of resin supported nanoiron and evaluation of efficiency for the remediation of Cr(VI) contaminated groundwater by batch tests. Bull Environ Contam Toxicol 101:711–717. https://doi.org/10.1007/s00128-018-2425-2

Vasileiou E, Papazotos P, Dimitrakopoulos D, Perraki M (2019) Expounding the origin of chromium in groundwater of the Sarigkiol basin, Western Macedonia, Greece: a cohesive statistical approach and hydrochemical study. Environ Monit Assess 191:509

Vilardi G, Ochando-pulido JM, Stoller M et al (2018) Fenton oxidation and chromium recovery from tannery wastewater by means of iron-based coated biomass as heterogeneous catalyst in fi xed-bed columns. Chem Eng J 351:1–11. https://doi.org/10.1016/j.cej.2018.06.095

Xie B, Zuo J, Gan L et al (2014) Cation exchange resin supported nanoscale zero-valent iron for removal of phosphorus in rainwater runoff. Front Environ Sci Eng 8:463–470. https://doi.org/10.1007/s11783-013-0575-3